# Analysis for Scattering of Non-homogeneous Medium by Time Domain Volume Shooting and Bouncing Rays

**Jun Li, Huaguang Bao, and Dazhi Ding**

School of Electronic and Optical Engineering
Nanjing University of Science and Technology, Nanjing, Jiangsu Province 210094, China
hgbao@nujst.edu.cn

***Abstract*** ─ In order to evaluate scattering from hypersonic vehicles covered with the plasma efficiently, time domain volume shooting and bouncing rays (TDVSBR) is first introduced in this paper. The new method is applied to solve the transient electromagnetic scattering from complex targets, which combines with non-homogeneous dielectric and perfect electric conducting (PEC) bodies. To simplify the problem, objects are discretized into tetrahedrons with different electromagnetic parameters. Then the reflection and transmission coefficients can be obtained by using theory of electromagnetic waves propagation in lossy medium. After that, we simulate the reflection and transmission of rays in different media. At last, the scattered fields or radiation are solved by the last exiting ray from the target. Compared with frequency-domain methods, time-domain methods can obtain the wideband RCS efficiently. Several numerical results are given to demonstrate the high efficiency and accuracy of this proposed scheme.

***Index Terms*** ─ Non-homogeneous dielectric, time domain, Volume Shooting and Bouncing Rays (VSBR).

## I. INTRODUCTION

In recent years, with the application of short pulse ultra wideband (UWB) communication in target recognition and remote sensing, electromagnetic (EM) time domain analysis method has received more and more attention. All kinds of numerical methods in computational EM have been widely used in various fields. Especially, the time-domain high frequency approximation methods have attracted more and more attention in the scattering analysis of electrically large structures.

With the rapid development of computer technology, the simulation capability of full-wave methods have been improved greatly. But it is also tedious to solve scattering of large electrical structures with full-wave methods [1-3]. Therefore, it is significant for seeking a superior-efficiency method to analyze the scattering from electrically large structures. Moreover, high frequency approximation methods fulfill the requirements in this project. In fact, with the increasing electrically size of the target, mutual coupling effects between elements have been reduced gradually. Therefore, the results of the high frequency approximation methods are more and more close to results of full wave numerical methods. Above all, high frequency approximation methods have crucial values in engineering application for the rapid analysis of EM scattering of electrically large targets. Time-domain full wave methods include the Finite Difference Time Domain (FDTD) [4-6], the Time Domain Finite Element Method (FETD) [7,8], and the Time Domain Integral Equation Method (TDIE) [9,10], etc. One of the advantages for the above time domain numerical method is that accurate EM simulation results can be obtained from the targets with complex shapes and materials. However, the above methods also have their own defects [11]. For example, the cumulative error of time stepping, the truncation error of spatial sampling and the numerical error of the radiation boundary condition. Meanwhile, time-domain full wave methods mentioned above have a common fatal defect: when the electric size of the scattering/radiation target is large, they all have a great demand on computer memory and are time-consuming. In contrast, the time domain high frequency approximation methods are the best effective way to solve the above issues. Compared with time-domain full wave methods, the advantages of time-domain high frequency approximation methods are remarkable. They cost less computing memory but have fast computing speed. According to different situations, time domain high frequency approximation methods can also combine with time domain full wave methods [12,13]. At present, it is common to analyze perfect electrically conducting (PEC) and homogeneous medium through high frequency approximation methods. For PEC or homogeneous medium, we usually use Physical Optics (PO) or Shooting and Bouncing Rays (SBR) to analyze the scattering or radiation of targets [14-16]. For non-homogeneous medium, such as plasma, the plasma sheath is equivalent to layered homogeneous dielectric in high frequency approximation methods

*Submitted On: May 6, 2020*
*Accepted On: December 6, 2020*
https://doi.org/10.47037/2020.ACES.J.360303

[17,18]. Obtaining the reflection coefficient of plasma sheath by recursion formulas. However, if the situation is complicated that the speed of hypersonic vehicles reached more than 10 Mach. Then the aircraft sheath electron obvious change causes dielectric constant change irregularly. Time domain full wave methods cannot solve hypersonic vehicles efficiently. As a result, we urgently need a new method to solve this problem.

In this paper, a novel method is proposed to analyze the scattering of objects, which are combined with non-homogeneous medium and PEC bodies. When the rays are propagating in non-homogeneous medium, they transmit and reflect on the interface of different medium. After multiple reflection and refraction, the rays leave objects and finally the far field integration is calculated by the principle of Physical Optics. The paper is organized as follows. Section II contains EM computing formulas of TDVSBR in detail. In Section III. numerical examples demonstrating the accuracy and efficiency of the method are presented. In Section IV, we conclude the advantages of the new method in solving the scattering of non-homogeneous dielectric and metal mixed target.

## II. THEORY AND FORMULATION

### A. Shooting and Bouncing Ray (VSBR) modeling framework involving dielectrics and perfect conductors

The main task of the spread of wave in dielectrics in an SBR based approach is to calculate the reflected and transmitted waves at material interfaces. In most case, the wave will generate nonuniform wave when wave transmitted between the nonuniform lossy medium. It means the directions of constant phase and amplitude plane of the wave are not identical, and there is an angle $0 \le \rho \le \pi/2$ between them (for uniform wave $\rho$=0 ). Similar to [19], the scenario to investigate is shown in Fig. 1, where a nonuniform wave propagates from medium 1 to medium 2. The complex propagation vector $\gamma$ can be generally represented as $\gamma=\alpha+j\beta$ with $\alpha$ represents the amplitude vector and $\beta$ represents the phase vector. In [20], the relevant work of solving the reflection and transmission coefficients of the nonuiform wave propagates in the nonuiform medium is presented.

The propagation vector in medium i can be express in real-angle form as:

$$\begin{aligned}\gamma_i=&\alpha_i\left(\sin\varsigma_i\hat{e}_x+\cos\varsigma_i\hat{e}_z\right)\\&+j\beta_i\left(\sin\xi_i\hat{e}_x+\cos\xi_i\hat{e}_z\right)\end{aligned}, \tag{1}$$

where $\varsigma_i=\xi_i+\rho_i$ and $i=1,2$ .

The intrinsic propagation constant of medium i is only determined by the properties of material, which can be expressed by:

$$\begin{aligned}\gamma_{0i}&=\alpha_{0i}+j\beta_{0i}=jk_0\sqrt{\varepsilon_{ri}\mu_{ri}}\\&=\frac{\omega}{c}\sqrt{|\varepsilon_{ri}||\mu_{ri}|}\left(\sin\sigma+j\cos\sigma\right)\end{aligned}, \tag{2}$$

where $\alpha_{0i}=\frac{\sqrt{\varepsilon_{ri}\mu_{ri}}}{c}sin\sigma$ , $\beta_{0i}=\frac{\sqrt{\varepsilon_{ri}\mu_{ri}}}{c}cos\sigma$ .

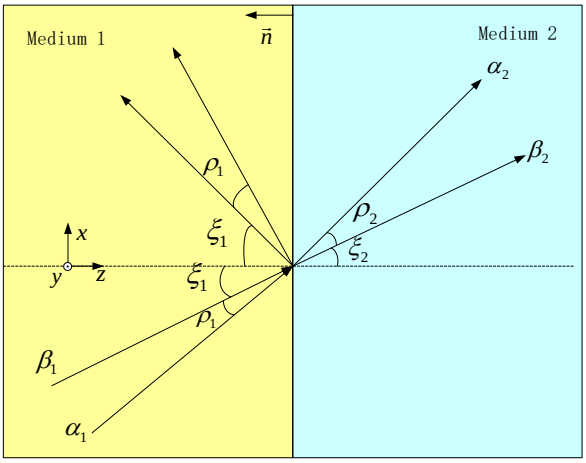


Fig. 1. Angles and directions to describe the wave propagation at the transition of two lossy media.

According to phase continuity at the interface of the two media and the law of Snell, we can obtain:

$$\alpha_1=\sqrt{\frac{\beta_{01}^2-\alpha_{01}^2}{2}}\cdot\sqrt{\sqrt{1+\left(\frac{2\alpha_{01}\beta_{01}}{\left(\beta_{01}^2-\alpha_{01}^2\right)\cos\rho_1}\right)^2}-1}, \tag{3}$$

$$\beta_1=\sqrt{\frac{\beta_{01}^2-\alpha_{01}^2}{2}}\cdot\sqrt{\sqrt{1+\left(\frac{2\alpha_{01}\beta_{01}}{\left(\beta_{01}^2-\alpha_{01}^2\right)\cos\rho_1}\right)^2}+1}. \tag{4}$$

By defining:

$$\gamma_{1t}=\alpha_1\sin\varsigma_1+j\beta_1\sin\xi_1. \tag{5}$$

We can obtain:

$$\alpha_2=\sqrt{\frac{1}{2}\left(\left|\gamma_{1t}\right|^2+\mathrm{Re}\left(\gamma_{02}^2\right)+\left|\gamma_{1t}^2-\gamma_{02}^2\right|\right)}, \tag{6}$$

$$\beta_2=\sqrt{\frac{1}{2}\left(\left|\gamma_{1t}\right|^2-\mathrm{Re}\left(\gamma_{02}^2\right)+\left|\gamma_{1t}^2-\gamma_{02}^2\right|\right)}. \tag{7}$$

For TE polarization, we obtain:

$$R_{TE}=\frac{\mu_2A_1-\mu_1A_2}{\mu_2A_1+\mu_1A_2}, \tag{8}$$

$$T_{TE} = \frac{2\mu_2 A_1}{\mu_2 A_1 + \mu_1 A_2}, \tag{9}$$

where $A_1 = \alpha_1 \cos\varsigma_1 + j\beta_1 \cos\xi_1$ and $A_2 = \alpha_2 \cos\varsigma_2 + j\beta_2 \cos\xi_2$.

$R$ represents the reflection coefficient and $T$ represents the transmission coefficient. From the expression, there is no relationship between the reflection coefficient and the frequency of incident wave. So is the transmission coefficient.

In the same way, for TM polarization, we obtain:

$$R_{TM} = \frac{-\varepsilon_2 A_1 + \varepsilon_1 A_2}{\varepsilon_2 A_1 + \varepsilon_1 A_2}, \tag{10}$$

$$T_{TM} = \frac{2\varepsilon_2 A_1}{\varepsilon_2 A_1 + \varepsilon_1 A_2}. \tag{11}$$

According to reflection and transmission coefficient, we can achieve the reflection and transmission field. To calculate the scattered far field, we not only need the equivalent electric currents, but also need the equivalent magnetic currents. According to the Stratton-Chu formula, we deduce the scattered far field of physical optics. The scattered far field is obtained by accumulation of the electric current and the magnetic current contributions.

**B. Calculation of broadband RCS**

When the rays comes from the air into the medium, the total field on the surface is as followed:

$$\vec{E} = \vec{E}^i + \vec{E}^r, \tag{12}$$

$$\vec{H} = \vec{H}^i + \vec{H}^r. \tag{13}$$

$\vec{E}$ and $\vec{H}$ represent the total electric and magnetic field on the surface of the object respectively. *i* represent the incident and *r* represent the reflection. The far field is obtained by solving the current and magnetic current on the surface of the medium.

$\vec{E}^i\left(\vec{r}',t\right)$ is the time series of the incident electric field when it intersects with the target at the last time:

$$\vec{E}^i\left(\vec{r}',t\right) = \vec{e}_0^i\left(\vec{r}',t\right)s(t), \tag{14}$$

where $s(t)$ represents the incident pulse. It is known from the Fourier transform that the frequency domain multiplication corresponds to the convolution of the time domain:

$$\vec{E}_J^s(\vec{r},t) = \frac{1}{4\pi rc}\hat{s}\times\int_s \hat{s}\times\left\{\hat{n}\times\left[\begin{array}{l} k_i\times\vec{e}_0^i\left(\vec{r}',t\right) \\ +k_s\times\left(\overline{\overline{R}}(t)*\vec{e}_0^i\left(\vec{r}',t\right)\right)\end{array}\right]\right\} \times\frac{\partial}{\partial t}s\left(t-t_d\right)ds, \tag{15}$$

$$\vec{E}_M^s(\vec{r},t) = -\frac{1}{4\pi rc}\hat{s}\times\int_s \hat{n}\times\left[\begin{array}{l}\vec{e}_0^i\left(\vec{r}',t\right) \\ +\left(\overline{\overline{R}}(t)*\vec{e}_0^i\left(\vec{r}',t\right)\right)\end{array}\right]\frac{\partial}{\partial t}s\left(t-t_d\right)ds, \tag{16}$$

$$\vec{E}^s(\vec{r},t) = \vec{E}_J^s(\vec{r},t) + \vec{E}_M^s(\vec{r},t), \tag{17}$$

where $Z_0$ represents the wave impedance of free space, $\vec{r}$ is the position vector of the observation point and $\vec{r}'$ is position vector of any element of the target surface. *r* represents the distance from surface element to observation point, $\hat{n}$ is the unit normal vector of the surface element. $t_d = \left(\hat{i}\cdot\vec{r}_0 - \hat{s}\cdot\vec{r}'\right)/c$ represents the time delay. The time domain response sequence is transformed by discrete Fourier transform, and the corresponding frequency response sequence can be obtained. Finally, we will obtain the broadband RCS, after the frequency domain response sequence is divided by the frequency domain sequence of the incident pulse signal.

When the rays emitted from the medium into the air, the total field on the surface is as followed:

$$\vec{E} = \vec{E}^t, \tag{18}$$

$$\vec{H} = \vec{H}^t, \tag{19}$$

$$\vec{H}^t = \frac{1}{Z_0}\left(k_t\times\vec{E}^t\right), \tag{20}$$

where $k_t$ represents the direction of transmission of rays.

$\vec{E}^i\left(\vec{r}',t\right)$ represents the time series of the transmission electric field out of the target:

$$\vec{E}^t\left(\vec{r}',t\right) = \vec{e}_0^t\left(\vec{r}',t\right)s(t), \tag{21}$$

$$\vec{E}_J^s(\vec{r},t) = \frac{1}{4\pi rc}\hat{s}\times\int_s \hat{s}\times\left\{\hat{n}\times\left[k_t\times\vec{e}_0^{\,t}\left(\vec{r}',t\right)\right]\right\} \cdot\frac{\partial}{\partial t}s\left(t-t_d\right)ds, \tag{22}$$

$$\vec{E}_M^s(\vec{r},t) = -\frac{1}{4\pi rc}\hat{s}\times\int_s \hat{n}\times\vec{e}_0^{\,t}\left(\vec{r}',t\right)\frac{\partial}{\partial t}s\left(t-t_d\right)ds, \tag{23}$$

$$\vec{E}^s(\vec{r},t) = \vec{E}_J^s(\vec{r},t) + \vec{E}_M^s(\vec{r},t). \tag{24}$$

## III. NUMERICAL RESULTS

The first example and the second example are carried out on the computer of Intel(R) Core(TM)2 Quad CPU Q9500 equipped with 8GB RAM at 2.83GHz and the edition of FEKO is 7.0. TDVSBR and FDVSBR are coded by FORTRAN. This is a big cube which is made up of 8 smaller cubes and the length of each small cube is 0.2m in Fig. 2. When the frequency is 3 GHz, the relative dielectric constant and electrical conductivity of

the dark cubes are respectively $\varepsilon_r = 0.95$, $\sigma = 0.067$. The light cubes are $\varepsilon_r = 0.8$, $\sigma = 0.085$. The permeability $\mu_r$ of them are (1.0,0). The center frequency of the incident pulse is $f_0 = 2$ GHz, and the effective frequency band of the calculation is $1 \sim 3$ GHz. The direction of incidence of the pulse is $\theta = 45°$, $\varphi = 0°$.

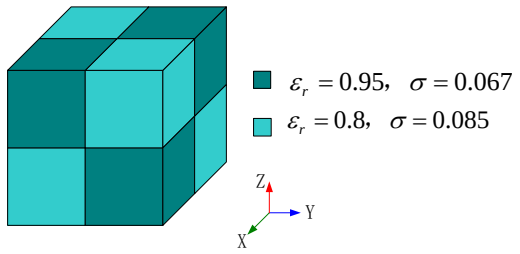


Fig. 2. Non-homogeneous medium cubes.

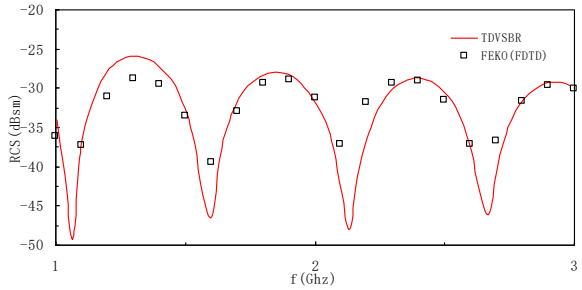


Fig. 3. Broadband monostatic RCS(VV) of non-homogeneous medium cube.

Table 1: The efficiency of different methods

| | **TDVSBR** | **FEKO(FDTD)** |
|---|---|---|
| Time(s) | 5 | 1282 |
| Memory (MB) | 4.8 | 191 |

The result of TDVSBR and FEKO make a good agreement in Fig. 3. Table 1 shows that the time of FEKO(FDTD) is about 256 times slower than TDVSBR in first example. TDVSBR has great advantages than FEKO(FDTD).

The second example shows a complex mixed target of rectangular metal cavity (6m*6m*10m) and non-homogeneous dielectric (3m*3m*2m) in Fig. 4. Dielectric parameters and permeability of the light purple rectangular are $\varepsilon_r = 4$, $\sigma = 0.033$ and deep purple rectangular are $\varepsilon_r = 5$, $\sigma = 0.0825$. $\theta = 15°, \varphi = 0°$ is the incidence direction and observation direction.

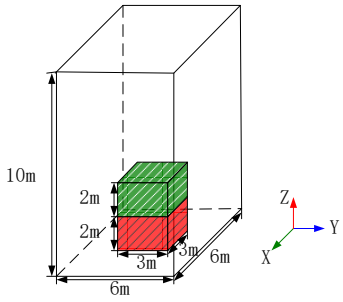


Fig. 4. A complex mixed target of rectangular metal cavity and non-homogeneous dielectric.

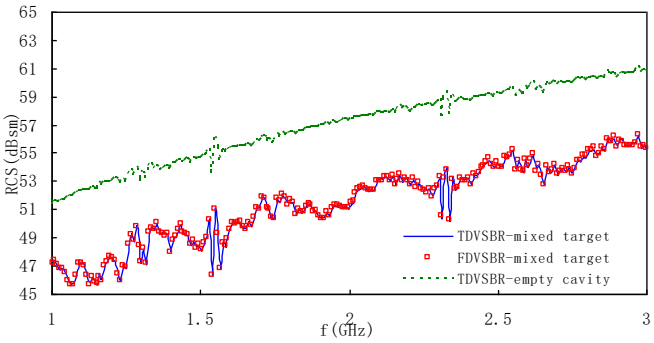


Fig. 5. The broadband monostatic RCS(vv) of empty cavity and the combined target.

In Fig. 5, the RCS of combined target is higher than the empty cavity and the gap reaches more than 10dB. Because of the electric size of the target is too large, we need to use subdivision technique to increase the efficiency of the new method. We use the corresponding gird of 300MHz to fit the shape of the mixed target, and subdivide the gird 3 times through the subdivision technique. The time-consuming of TDVSBR is 198s, and the memory of it is about 10 MB.

The third example is shown in Fig. 6, It calculates the broadband RCS of a metal warhead at a height of 30km and a speed of 10 Maher. The radius of warhead is 0.1m and the length is 0.2m. The plasma sheath radius of the ionized plasma is 0.4m and the length is 0.6m. the central frequency of the incident pulse is $f_0 = 6$ GHz, and the effective frequency band of the calculation is from 3 to 12GHz. The direction of incidence of the pulse is $\theta = 90°$, $\varphi = 0°$. In this method, we consume the relative dielectric constant and electrical conductivity are constant at center frequency of the interested frequency band. When the dispersion effect is obvious, this method has its disadvantages.

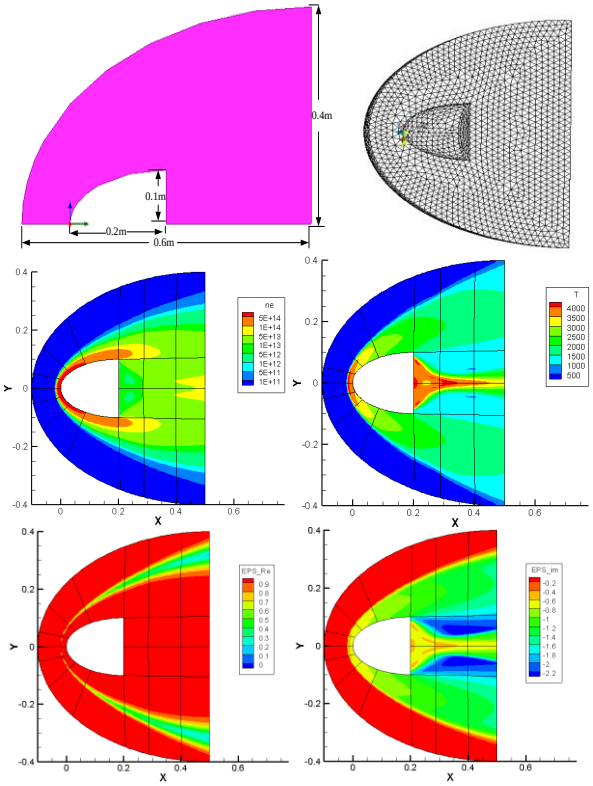


Fig. 6. The model of plasma sheath.

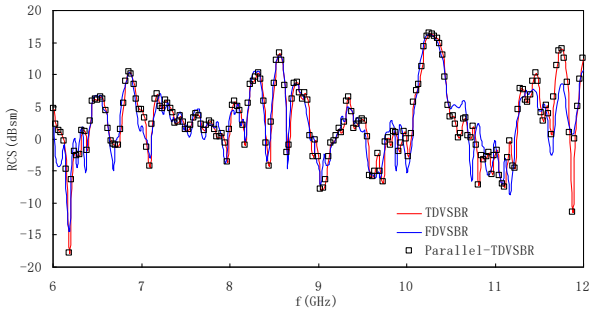


Fig. 7. Broadband monostatic RCS(vv) of plasma sheath.

In Fig. 7, the result of TDVSBR and FDVSBR are in good agreement. We do not consider the despersion of the plasma in TDVSBR. Strictly writing, the despersion of the plasma has effect on the way of the propagation of the rays. If ways have always change with the time. Then TDVSBR has to trace the path of the rays at every point of time. It must time-consuming and we do not accept this TDVSBR. Therefore, we weaken the influence of despersion on plasma. In our work, $\varepsilon_r$, $\mu_r$ and $\sigma$ of dielectric are fixed value. The value of three parameters are selected at the center frequency. In FDVSBR, $\varepsilon_r$, $\mu_r$ and $\sigma$ of dielectric in plasma sheath change with the frequency of the incident. However, in TDVSBR, when the frequency of the incident is changing, $\varepsilon_r$, $\mu_r$ and $\sigma$ of dielectric in plasma sheath are fixed. When the band of incident is not wide, $\varepsilon_r$, $\mu_r$ and $\sigma$ of dielectric in plasma sheath have little impact on RCS at different frequency of the incident. $\varepsilon_r$, $\mu_r$ have influence on the way of the ray. If the way of the ray changes at different frequencies of incident, TDVSBR would time-consuming and lose the its advantage. For convenience, we fix $\varepsilon_r$, $\mu_r$ and $\sigma$ of dielectric in plasma sheath at different frequencies of incident.

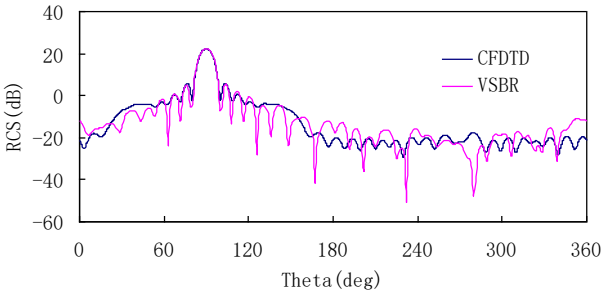


Fig. 8. Bistatic RCS(vv) of plasma sheath at 3GHz.

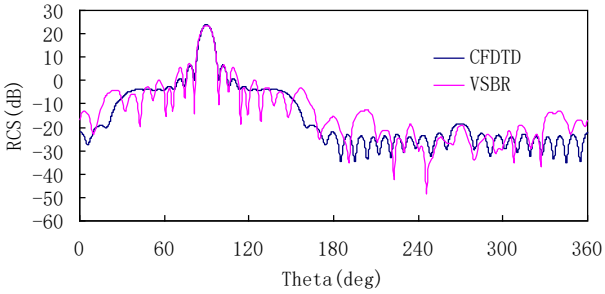


Fig. 9. Bistatic RCS(vv) of plasma sheath at 3.5GHz.

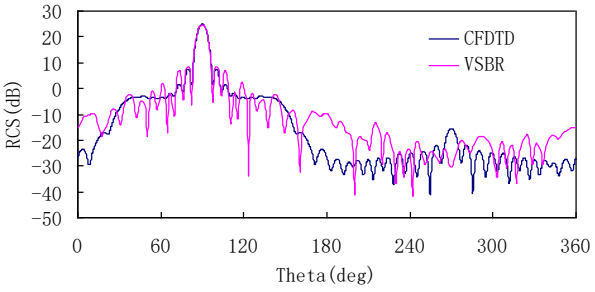


Fig. 10. Bistatic RCS(vv) of plasma sheath at 4GHz.

In Fig. 8, Fig. 9 and Fig. 10, observation range is $\varphi = 0°$, $\theta = 0 \sim 360°$. The results of CFDTD and TDVSBR are in good agreement. $\varepsilon_r$, $\mu_r$ and $\sigma$ of plasma has little effect on the scattering, therefore we

use TDVSBR to evaluate the the scattering of plasma.

As shown in Fig. 11, the time domain response of CFDTD and TDVSBR has a good agreement at the observation point (100m,0,0). In order to simulate electromagnetic characteristics of plasma sheath conveniently, researchers commonly use different medium to simulate plasma sheath.

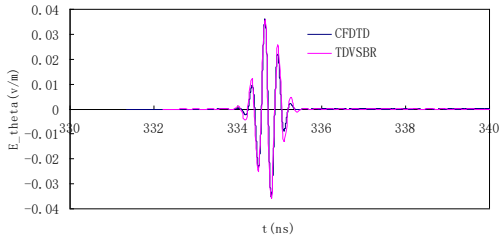


Fig. 11. The time domain response of plasma sheath at (100m,0,0).

As shown in Table 2, TDVSBR has great advantages than full wave methods in analyze of electrical large plasma sheath. TDVSBR costs less memory and has higher computing speed than CFDTD.

Table 2: The comparison of computational efficiency between the CFDTD method and TDVSBR method, and the two methods are used on a single CPU code

| | **TDVSBR** | **CFDTD** |
|---|---|---|
| Time(h) | 0.24 | 80 |
| Memory(G) | 1.2 | 30 |

## IV. CONCLUSION

A novel high frequency approximation method based on SBR to calculate the scattering of non-homogeneous dielectric and metal mixed target is presented. According to the time and memory consumption, the new method is more efficient than accurate method, and the accuracy of the new method is acceptable. An important breakthrough of the new method in high approximation method is to calculate the non-homogeneous dielectric and metal mixed target, especially the complex target, such as hypersonic vehicle.

## ACKNOWLEDGMENT

This work was supported in part by Natural Science Foundation of 61931021, 61890541, National Key Lab of Science and Technology on space microwave under Grant 2018SSFNKLSMT-06, and Grant HTKJ2020KL504012, by the Fundamental Research Funds for the Central Universities No. 30918011202.

## REFERENCES

[1] L. Wang, M. Wang, K. Zhang, W. Cui, H. Zheng, and E. Li, "Three-dimensional spherical-shaped UPML for FDTD with cubic lattices," *Applied Computational Electromagnetics Society Journal*, vol. 34, no. 3, pp. 425-433, 2019.

[2] J. Cao, R. S. Chen, Y. L. Hu, and S. F. Tao, "A higher order Nyström scheme for marching-on-in-time solution of time-domain integral equation," *IEEE Trans. Antennas Propagat.*, vol. 63, pp. 2762-2767, 2015.

[3] Y. L. Hu and R. S. Chen, "Analysis of scattering from composite conducting dispersive dielectric objects by Time-domain volume-surface integral equation," *IEEE Trans. Antennas Propagat.*, vol. 64, pp. 1984-1989, 2016.

[4] J. G. Maloney, G. S. Smith, and W. R. Scott, "Accurate computation of the radiation from simple antennas using the finite-difference time-domain method," *IEEE Trans. Antennas Propagat.*, vol. 38, pp. 1059-1068, 1990.

[1] H. Bao and R. Chen, "An efficient domain decomposition parallel scheme for leapfrog ADI-FDTD method," *IEEE Trans. Antennas Propagat.*, vol. 65, pp. 1490-1494, 2017.

[5] Z. Sun, L. Shi, Y. Zhou, B. Yang, and W. Jiang, "FDTD evaluation of LEMP considering the lossy dispersive ground," *Applied Computational Electromagnetics Society Journal*, vol. 33, no. 1, pp. 4-17, 2018.

[6] M. Dong, J. Chen, and A. Zhang, "A convolutional perfectly matched layer (CPML) for the fourth-order one-step leapfrog HIE-FDTD method," *Applied Computational Electromagnetics Society Journal*, vol. 33, no. 1, pp. 1-6, 2018.

[7] Z. Lou and J.-M. Jin, "Modeling and simulation of broad-band antennas using the time-domain finite element method," *IEEE Trans. Antennas Propagat.*, vol. 53, pp. 4099-4110, 2005.

[8] Y. L. Hu and R. S. Chen, "Hybridization of curvilinear time-domain integral equation and time-domain optical methods for electromagnetic scattering analysis," *IEEE Trans. Antennas Propagat.*, vol. 46, pp. 318-324, 1998.

[9] S. P. Walker and C. Y. Leung, "Parallel computation of time-domain integral equation analyses of electromagnetic scattering and RCS," *IEEE Trans. Antennas Propagat.*, vol. 45, pp. 614-619, 1997.

[10] X. Zhou and T. J. Cui, "A closed-form representation of time-domain far fields based on physical optics," *IEEE Trans. Antennas Propagat.*, vol. 11, pp. 965-968, 2012.

[11] A. Altintas and P. Russer, "Time-domain equivalent edge currents for transient scattering," *IEEE Trans. Antennas Propag*., vol. 49, pp. 602-606, 2001.
[12] L. X. Yang, D. B. Ge, and B. Wei, "Time-domain physical-optics method for transient scattering analysis," *The 2006 4th Asia-Pacific Conference on Environmental Electromagnetics*, Dalian, China, pp. 861-864, 2006.
[13] A. Boag and C. Letrou, "Multilevel fast physical optics algorithm for radiation from non-planar apertures," *IEEE Trans. Antennas Propag*., vol. 53, pp. 2064-2072, 2005.
[14] C. Pienaar, J. W. Odendaal, J. C. Smit, J. Joubert, and J. E. Cilliers, "RCS results for an electrically large realistic model airframe," *Applied Computational Electromagnetics Society Journal*, vol. 45, pp. 87-90, 2018.
[15] D. Shi, X. Tang, C. Wang, M. Zhao, and Y. Gao, "A GPU implementation of a shooting and bouncing ray tracing method for radio wave propagation," *Applied Computational Electromagnetics Society Journal*, vol. 32, pp. 614-620, 2017.
[16] W. Wong and D Cheng, "High-frequency scattering from a conducting cylinder with an inhomogeneous plasma sheath," *IEEE Trans. Antennas Propag*., vol. 17, pp. 208-215, 1969.
[17] S. H. Liu and L. X. Guo, "Analyzing the electromagnetic scattering characteristics for 3-D inhomogeneous plasma sheath based on PO method," *IEEE Transactions on Plasma Science*, vol. 44, pp. 2838-2843, 2016.
[18] R. Radcliff and C. Balanis, "Modified propagation constants for nonuniform plane wave transmission through conducting media," *IEEE Trans. Geosci. Remote Sens*., vol. 20, pp. 408-411, 1982.
[19] J. Roy, "New results for the effective propagation constants of nonuniform plane waves at the planar interface of two lossy media," *IEEE Trans. Antennas Propag*., vol. 51, no. 6, pp. 1206-1215, 2003.
[20] R. Brem and T. F. Eibert, "A shooting and bouncing ray (SBR) modeling framework involving dielectrics and perfect conductors," *IEEE Trans. Antennas Propag*., vol. 63, no. 8, pp. 3599-3609, 2003.

**Jun Li** was born in Taizhou, China. He received the B.S. degree in Optical Engineering from the School of Electrical Engineering and Optical Technique, Zijin College of Nanjing University of Science and Technology, Nanjing, China, in 2013. He is currently pursuing his Ph.D. degree in Electronic Engineering at Nanjing University of Science and Technology. The interest of his research are antennas, high frequency method and computational electromagnetics.

**Huaguang Bao** received the B.S. and Ph.D. degrees in Electromagnetic Field and Microwave Technique from Nanjing University of Science and Technology (NUST), Nanjing, China, in 2011 and 2017, respectively. In 2017, he was a Post-Doctoral Scholar with the Computational Electromagnetics and Antennas Research Laboratory, Department of Electrical Engineering, Pennsylvania State University, University Park, PA, USA. He is currently an Associate Professor with the Electronic Engineering of NJUST. His research interests include semiconductor simulation, RF-integrated circuits, and computational electromagnetics.

**Dazhi Ding** was born in Jiangsu, China, in 1979. He received the B.S. and Ph.D. degrees in Electromagnetic Field and Microwave Technique from Nanjing University of Science and Technology (NUST), Nanjing, China, in 2002 and 2007, respectively. During 2005, he was with the Center of Wireless Communication in the City University of Hong Kong, Kowloon, as a Research Assistant. He is currently an Associate Professor with the Electronic Engineering of NJUST. He is the author or co-author of over 30 technical papers. His current research interests include computational electromagnetics, electromagnetic scattering, and radiation.